FEASIBILITY OF PLASMONIC CIRCUITS MERGED WITH SILICON INTEGRATED CIRCUITS

Mitsuo Fukuda, Ph.D*, Yuta Tonooka, M.E., and Yasuhiko Ishikawa, Ph.D
Toyohashi University of Technology
Toyohashi, Aichi, Japan
*fukuda@ee.tut.ac.jp

ABSTRACT

Plasmonic signal transmission via nanoscale plasmonic waveguides is a new technique with the potential to increase the information transfer capacity in silicon integrated circuits (ICs). During propagation, surface plasmon polaritons (SPPs) exhibit characteristics of a lightwave whose transmission loss is mainly determined by the collective oscillation of electrons. Using this lightwave aspect of SPPs, information can be transmitted using plasmonic signals and optical transmission circuits and networks can be built at the micro/nanoscale. This size scale correlates well with that of electronic circuits comprising metal-oxide-semiconductor field-effect transistors (MOSFETs). In this article, the feasibility of on-chip interconnects and other circuits were discussed and confirmed on the basis of previously developed plasmonic components.

The first example examined herein was a wavelength-division-multiplexing circuit comprising a multiplexer and demultiplexer (in 1310 and 1550 nm-wavelength bands), discussed based on the experimental results for each component. Multiplexed signals at the multiplexer were guided into a single-mode waveguide, divided at the demultiplexer and then passed to the electronic circuits. The transmitted plasmonic signals were converted to electric signals at the slits etched on the gate electrode, thereby driving the MOSFET without photodetectors, whereupon the MOSFET-amplified signals were outputted to the electronic circuits. The second example was coherent signal transmission via plasmonic circuits. The signal transmission was performed using micro/nanoscale plasmonic circuits in a manner similar to those of optical fiber transmission systems. These coherent signal transmissions via plasmonic signals were experimentally confirmed, being detected and converted to electric signals at the slits etched on the gate electrode of the MOSFET and then outputted therefrom. These experimental examples confirmed the feasibility of plasmonic circuits integrated with MOSFETs.

In plasmonic circuits, signal transmission loss is generally high compared to that of electric and lightwave signals. Herein, it was numerically confirmed again that the plasmonic signal transmission losses were lower than those of electric signals transmitted in electric circuits for plasmonic circuits not exceeding an area of a few hundred square micrometers. The loss of lightwave signals (e.g., transmitted in silicon waveguides) was much lower than those of plasmonic signals. However, as the waveguide width approached the cut-off wavelength, the loss quickly increased to be greater than that of plasmonic signals. This work indicates that plasmonic circuits have an advantage in nanoscale circuits. The circuits presented herein are currently too primitive for actual silicon IC applications, but are adequate to indicate the feasibility of merging plasmonic circuits with silicon ICs.

Keywords: surface plasmon polariton, plasmonic circuit, on-chip interconnect, integrated circuit, CMOS

INTRODUCTION

Recently, high-speed on-chip interconnects have been increasingly required to improve silicon integrated circuit (IC) performances and to match the potentially enormous information processing requirements. Optical techniques offer solutions to improve IC performance, and optical on-chip interconnects are being introduced into silicon ICs, while silicon waveguides for lightwave signal propagation are actively being developed to deal with the huge amounts of information needed to be processed. Among the possible optical techniques, a plasmonic circuit using surface plasmon polaritons (SPPs) as the signal is attractive because the resulting optical circuit can be on a smaller scale than that of lightwave circuits [1]−[5]. However, SPP signals are still comparatively primitive and their transmission losses are normally considered to be much higher than that of lightwaves.

Regarding transmission losses, we have previously reported that plasmonic circuits via waveguides composed of SiO_2 stripes on a metal film (i.e., dielectric-loaded surface plasmon (DLSP) waveguides)) exhibit relatively low losses compared with electrical circuits if the plasmonic circuits are less than a few hundred square micrometers in area [6]. For plasmonic circuits merged with silicon ICs, we have previously developed some plasmonic waveguides and components such as a plasmonic waveguide-integrated metal-oxide-semiconductor field-effect transistor (MOSFET) [7], [8], multiplexer [9], demultiplexer [10], crossing waveguide [11], propagation speed controller [12], and half adder

[13]. The propagation characteristics of plasmonic signals along plasmonic waveguides have also been studied [6], [14]. Based on these previously-developed plasmonic components, this article reviews and discusses the feasibility of plasmonic circuits merged with silicon ICs.

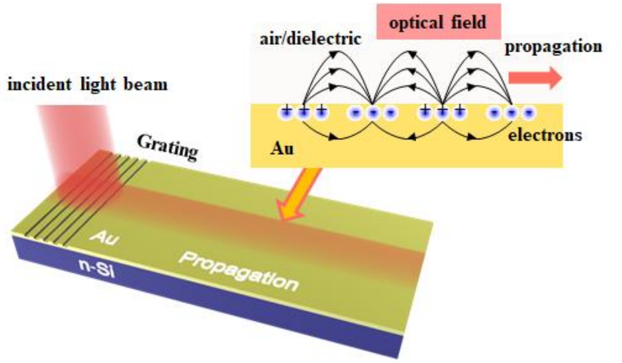

Figure 1. Schematic diagram of SPPs and their propagation.

CONCEPT OF PLASMONIC CIRCUITS

As shown in Figure 1, SPPs include electromagnetic waves that propagate along the surface of a conductor (i.e., metal and heavily doped semiconductor), where the collective oscillation of electrons couples with the optical field at the nanoscale beyond the diffraction limit of propagating lightwaves. The SPPs have lightwave characteristics, thus making available various techniques developed in optical fiber transmission systems such as wavelength-division-multiplexing and coherent detection [15], [16]. To merge these plasmonic circuits with silicon ICs, the following items are defined:

(1) The materials used were limited to silicon, silicon oxide, and metals typically used in silicon ICs. For the latter, though Al is typically used in silicon ICs, Au was chosen here to exploit the stability of Au in the laboratory atmosphere and because Al and Au circuit performances are almost identical [6]. We note that Cu is also used in silicon ICs but the transmission loss was excessive in Cu waveguides because the SPP optical field deeply penetrates the Cu surface in the 1300 and 1550 nm-wavelength bands.

(2) The plasmonic waveguide and component structures were simplified as much as possible. Thus, the components were formed by combining only single- and multi-mode waveguides. The circuits comprising these components were fabricated simultaneously by patterning a mesa structure into an SiO_2 film deposited on a metal film, where the patterning was done using focused-ion-beam etching. (Here, nanoimprint lithography will be possible.) The waveguide formation process is shown in Figure 2.

(3) The used wavelengths were set at 1300 and 1550 nm-wavelength bands. These bands are transparent to silicon, thus suppressing noise induced by plasmonic signal absorption at any silicon parts. Further, these wavelength bands are used commercially in public optical fiber communication systems.

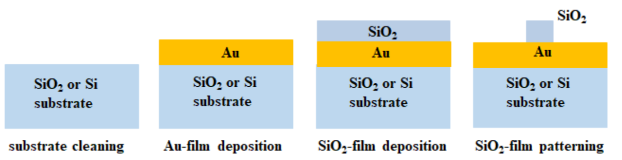

Figure 2. Fabrication procedure of plasmonic waveguides and components.

PLASMONIC WAVEGUIDES AND COMPONENTS

Single-mode waveguides were used as plasmonic waveguides, and thus their widths were in a range between 400 and 600 nm to facilitate low transmission loss and ease of fabrication. The width can be further reduced to a few tens of nanometers and plasmonic signals can still propagate on such narrow waveguides. The multimode waveguides acted as multimode interferometers (MMIs) and generated a spatial intensity distribution of the plasmonic signals via interference. The intensity distribution can be changed by varying the lengths and widths of the MMIs, and only plasmonic signals were guided to the output port set at the position corresponding to the high signal intensity domain. By combining these MMIs, multiplexing, demultiplexing, logic, and other performances could be obtained at light speed. The schematic diagrams and SEM images of the components fabricated are shown in Figures 3−7, and a brief description of each will be given in the following.

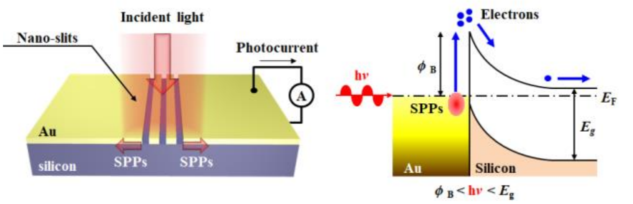

Figure 3. Schematic diagram of a plasmonic detector (left image) and the corresponding band diagram (right image).

(1) Detector (Figure 3) [17], [18]

Plasmonic signals can be easily detected with the photodetectors used in ordinary optical systems after the SPPs are converted to a propagating lightwave. Here, plasmonic signals were directly detected using slits etched in a metal film deposited on a silicon substrate, at whose interface a Schottky-type diode was formed. The detected light wavelength was determined by the Shcottky barrier height ϕ_B [19]−[22], where plasmonic signals in the 1300 and 1550 nm wavelength bands were detected herein. In plasmonic detectors, detection efficiency is enhanced by optimizing the pitch, width, and number of slits.

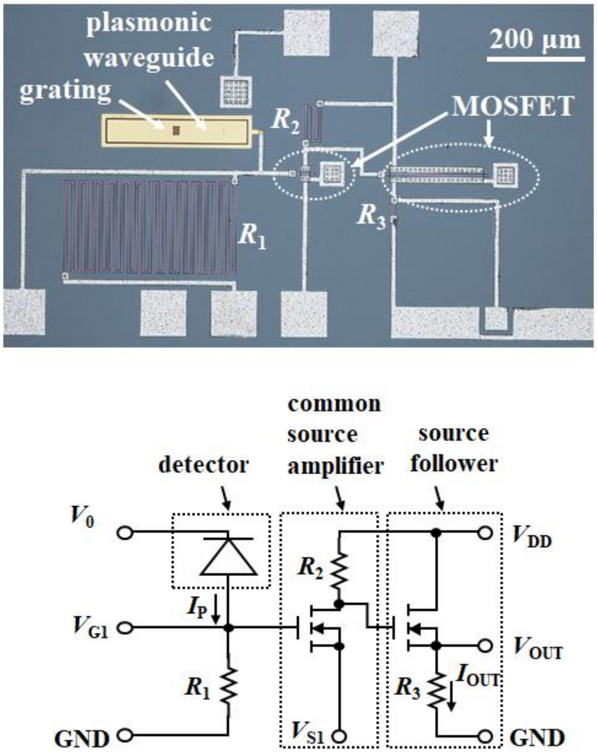

Figure 4. Detector-integrated MOSFET SEM image (top view) (upper image) and its circuit diagram (lower image).

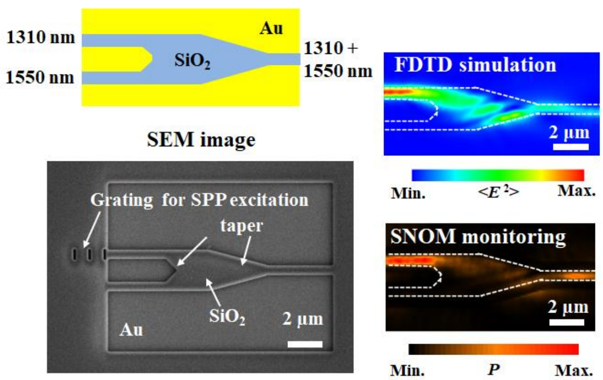

Figure 5. Multiplexer schematic (upper left) and SEM image (lower left) and its optical field distribution simulated by the finite-difference time-domain (FDTD) method (upper right) and experimentally obtained via scanning near-field microscope (SNOM) (lower right). The grating is set for only the 1300 nm-wavelength band in this sample.

(2) Detector-integrated MOSFET (Figure 4) [7], [8]

Owing to the simplicity of its structure and fabrication procedure, a plasmonic detector employing slits etched in a metal film was easily integrated with MOSFETs by forming slits on the gate electrode. The plasmonic waveguides were also integrated between the slit area and the gate electrode. Using these structures, the silicon MOSFETs were driven with plasmonic signals in the 1300 and 1550 nm-wavelength bands.

(3) Multiplexer (Figure 5) [9]

The multiplexer component multiplexes a few plasmonic signals possessing different wavelengths and outputs them to a single-mode plasmonic waveguide. This function can be obtained using the multimode waveguide as a MMI. The inputted signals are individually interfered and changed to a spatial intensity distribution so that each position of the peak intensity coincides with that of the output single-mode waveguide. The performance is similar to that of a coupler excepting the function of multiplexing different wavelength signals. The insertion loss was experimentally estimated to be less than 5.0 dB in both 1300 and 1550 nm-wavelength bands.

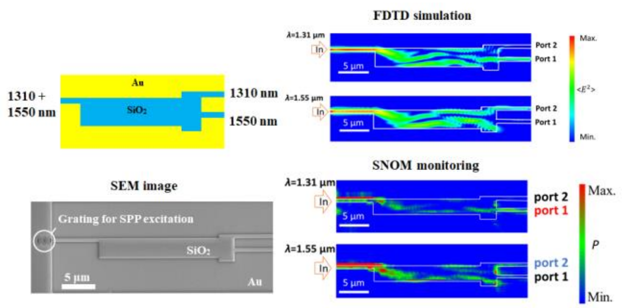

Figure 6. Demultiplexer schematic (upper left) and SEM image (lower left) and its optical field distribution simulated by FDTD method (upper right) and experimentally obtained via SNOM (lower right).

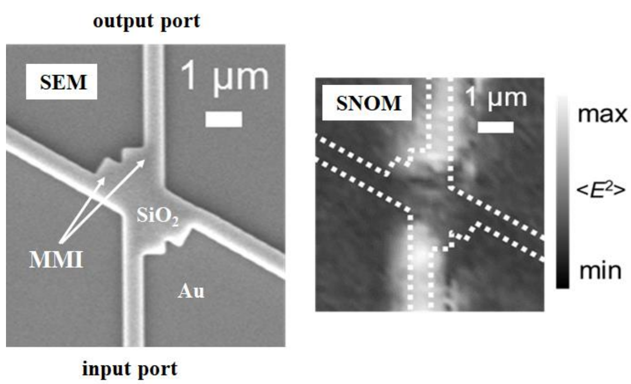

Figure 7. Crossing waveguide SEM image (left image) and optical intensity distribution obtained via SNOM (left image). Two MMIs are set at the crossing point.

(4) Demultiplexer (Figure 6) [10]

The demultiplexer component demultiplexes a few plasmonic signals possessing different wavelengths and outputs them to separate plasmonic waveguides. This function is the reverse of that of the multiplexer described in (3) above. The insertion loss was experimentally estimated to be approximately 4.3 and 8.9 dB in the 1300 and 1550 nm-wavelength bands, respectively.

(5) Crossing waveguide (Figure 7) [11]
The crossing waveguide in optical circuits for signal transmission has no meaningful corollary in electric circuits (i.e., wiring). In optical circuits, including plasmonic circuits, the propagation direction of plural signals can be controlled using a crossing waveguide [23], [24], although cross-talk can become a problem. The crossing waveguide typically exhibited a large loss and was not flexible for the crossing structure. However, these issues were solved to some extent by introducing two MMIs at the crossing point of two single-mode waveguides.

(6) Signal speed controller (slow light generator) [12]
Although its operation was experimentally confirmed, the signal speed control component remains in a primitive stage in our laboratory. When a waveguide is gradually narrowed, the SPP confinement within the waveguide is gradually enhanced during propagation. The SPPs can propagate along this type of narrowed waveguide without emission to the outside of the waveguide in a process called adiabatic nanofocusing or super focusing [25], [26]. At the narrow part of the waveguide the refractive index is high, and thus slow light is generated because the speed is inversely proportional to the refractive index. Using this slow light, the signal pulse width and transmission speed can be changed.

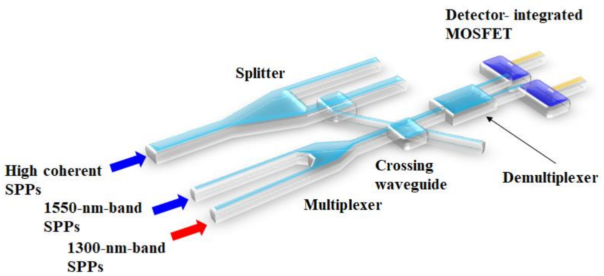

Figure 8. Schematic of part of a wavelength-division-multiplexing circuit in a plasmonic circuit, comprising a multiplexer, a crossing waveguide, a demultiplexer, and two detector-integrated MOSFETs.

(7) Logic circuit (half adder) [13]
The signal-phase information can be converted to an intensity distribution in waveguides, as described above. Using plasmonic signal interference, plasmonic logic circuits can be fabricated, although it remains primitive. These logic circuits were fabricated by combining only single- and multimode waveguides, and were linear systems operated as Boolean logic circuits. The performance of a half adder was experimentally confirmed.

PLASMONIC CIRCUITS AND SIGNAL TRANSMISSION TECHNIQUES

By combining the components described in the previous section, we can fabricate several functional plasmonic circuits. In this section, two plasmonic circuits are discussed.

(1) Wavelength-division-multiplexing circuit employing 1300 and 1550 nm-wavelength bands
Figure 8 shows a schematic diagram of a circuit, where a multiplexer and demultiplexer were connected with a single mode waveguide. Two plasmonic signals in the 1300 and 1550 nm-wavelength bands (i.e., transparent to silicon) were guided first to the multiplexer and then to the demultiplexer through the single-mode waveguide. The two signals separated at the demultiplexer were led to each gate electrode of the MOSFET through the waveguide and were then converted to electric signals at the plasmonic detector. These electric signals drove the MOSFETs. The single-mode waveguide in Figure 8 was formed with a 500 nm (width) × 500 nm (height) SiO_2 mesa structure fabricated on an Au film, with an estimated loss of 0.09 and 0.05 dB/μm in the 1300 and 1550 nm-wavelength bands [14], respectively. Circuits formed with the waveguides whose transmission lengths were less than 150 and 350 μm for the 1300 and 1550 nm-wavelength bands, respectively, possessed a transmission loss lower than those of electric signals in electronic circuits [6]. Using the experimental loss values for the primitive multiplexer and demultiplexer shown in Figures 5 and 6, the length of the single-mode waveguide between the multiplexer and demultiplexer can be set at ~100 μm and exhibit a lower loss than electronic circuits. These transmission losses will decrease as the plasmonic component design and process techniques advance in a manner similar to other electronic and photonic components. For the circuits, a MOSFET can be used for the detection of plasmonic signals, and the plasmonic signals can also be directly inputted to the gate electrode of a MOSFET [7], [8]. If electric isolation is required between the two output ports, isolation techniques using the native oxide will be applicable for the plasmonic signal [27]. These plasmonic circuits, therefore, are easily connected to electronic circuits.

(2) Coherent signal transmission through plasmonic circuits

We experimentally confirmed coherent signal transmission through plasmonic signals by detection of frequency-shift keying (FSK) combined with a self-delayed homodyne technique using a plasmonic circuit without a MOSFET [16]. In these experiments, the plasmonic circuit was essentially the same as that for intensity signal transmissions, though an additional light-beam incident system for generating beat signals was added. The schematic diagram of a circuit including a detector-integrated MOSFET is shown in Figure 9. A light beam outputted from the tunable laser was guided to a single-mode optical fiber and then divided to two optical paths. One was directly incident to the grating through the polarization controller 1 and was converted to plasmonic signals at the grating. The other was transmitted through a 7 km-long single-mode fiber and was incident to the grating through the polarization controller 2. The two plasmonic signals converted from the two light paths were then transmitted along a 50 μm-long waveguide and converted to electrical signals at the plasmonic detector.

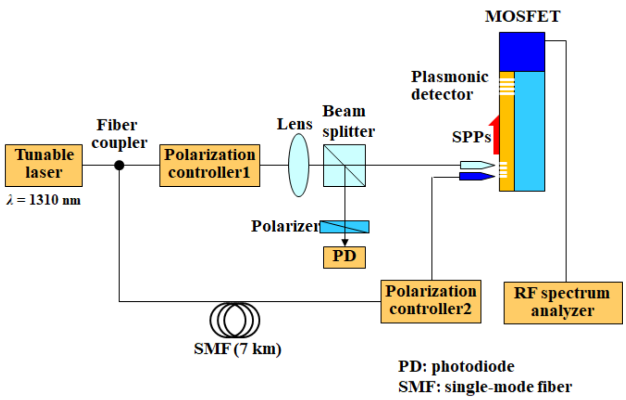

Figure 9. Block diagram of self-delayed homodyne detection system.

Figure 10 shows experimental data for an electric intensity spectrum and a beat spectrum as a function of frequency, both of which were outputted from an electronic circuit comprising MOSFETs. For the intensity signal transmission, a tunable laser beam modulated at 1 kHz was made incident to the grating, which converted it to plasmonic intensity signals. Here, the modulated light beam was not divided and was directly incident on the grating. The intensity modulation signal at 1 kHz was clearly observed in the electric signals (see Fig. 4). A homodyne beat signal with a peak at 0 Hz was also detected and outputted from the electronic circuit.

These wavelength-division-multiplexing and coherent detection circuits can be fabricated within an area a few hundred micrometers square, and the plasmonic signal losses are lower than those of electric signals within the same range [6]. Further, the transmission speed of plasmonic signals in plasmonic circuits are equal to the velocity of light.

This experimental validation of a wavelength-division-multiplexing circuit and a coherent system indicates the feasibility of plasmonic signal transmission through plasmonic circuits merged with silicon ICs.

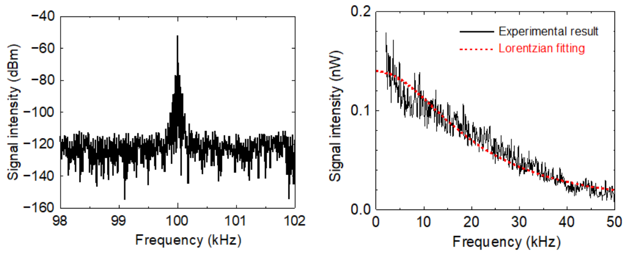

Figure 10. Output signals of a MOSFET of a plasmonic intensity signal modulated at 100 KHz (left image) and of a beat signal obtained from two plasmonic signals with equal wavelengths (i.e., frequencies) (right image). These spectra were observed with an rf spectrum analyzer.

SUMMARY

The feasibility of plasmonic circuits as applicable to silicon ICs was discussed on the basis of experimental data obtained for various previously-developed plasmonic components. We conclude that the plasmonic circuit can significantly increase the information processing speed of the silicon IC, as experimentally shown from the viewpoint of signal transmission speed and multiplex transmission.

ACKNOWLEDGMENTS

The authors thank Dr. Masashi Fukuhara, Tsukuba Research Center, Hamamatsu Photonics, K. K.; Dr. Takuma Aihara and Dr. Masashi Ota, NTT Science and Core Technology Laboratory Group, for their support and discussions on the design and fabrication of plasmonic components while enrolled in my laboratory. This work was supported by Japan Society for the Promotion of Science Grants-in-Aid for Scientific Research (KAKENHI) (Grant Nos. JP26289103, JP25630147, JP16K14253, and JP18K04282).

REFERENCES

[1] W. L. Barnes, A. Deleux, T. W. Ebbesen, “Surface plasmon subwavelength optics,” Nature, vol.424, pp. 824-830, 2003.
[2] T. W. Ebbesen, C. Genet, S. I. Bozhevolnyi, “Surface-plasmon circuitry,” Physics Today, May, pp. 44-50, 2008.
[3] D. A. B. Miller, “Optical interconnects to electronic chips,” Appl. Opt., vol.49, pp. F59-F70, 2010.
[4] M. L. Brongersma, L. M. Shalaev, “The case for plasmonics,” Science, vol.328, pp. 440-441, 2010.
[5] A. V. Krasavin and A. V. Zayats, “Benchmarking system-level performance of passive and active plasmonic

components: integrated circuit approach," Proc. of IEEE, vol. 104, pp. 2338-2348, 2016.
[6] M. Fukuda, Y. Tonooka, T. Inoue, M. Ota, "Feasibility of plasmonic circuits for on-chip interconnects," Solid-State Electron. vol. 156, pp. 33-40, 2019.
[7] T. Aihara, M. Fukuhara, A. Takeda, B. Lim, M. Futagawa, Y. Ishii, K. Sawada, M. Fukuda, "Monolithic Integration of Surface Plasmon Detector and Metal-Oxide-Semiconductor Field-Effect Transistors," IEEE Photon. J., vol. 5, Art. No. 6800609, 2013.
[8] H. Sakai, S. Okahisa, Y. Nakayama, K. Nakayama, M. Fukuhara, Y. Kimura, Y. Ishii, M. Fukuda, "Plasmonic and electronic device-based integrated circuits and their characteristics," Solid-State Electron., vol. 125, pp. 240-246, 2016.
[9] A. Sumimura, M. Ota, K. Nakayama, M. Ito, Y. Ishii, M. Fukuda, "Low-Return-Loss Plasmonic Multiplexer with Tapered Structure," IEEE Photon. Technol. Lett., vol. 28, pp. 2419-2422, 2016.
[10] K. Nakayama, Y. Tonooka, M. Ota, Y. Ishii, M. Fukuda, "Passive Plasmonic Demultiplexers Using Multimode Interference," J. Lightwave Technol., vol. 36, pp. 1979-1984, 2018.
[11] M. Ota, M. Fukuhara, A. Sumimura, M. Ito, T. Aihara, Y. Ishii, and M. Fukuda, "Dielectric-loaded surface plasmon polariton crossing waveguides using multimode interference," Opt. Lett., vol.40, pp. 2269-2272, 2015.
[12] T. Furuki, M. Ota, M. Fukuda, "Plasmonic slow light device using superfocusing on a bow-tied metallic waveguide," Opt. Lett., vol. 43, pp. 3232-3235, 2018.
[13] M. Ota, A. Sumimura, M. Fukuhara, Y. Ishii, and M. Fukuda, "Plasmonic-multimode-interference-based logic circuit with simple phase adjustment," Scientific Rep., vol. 6, Art. No. 24546, 2016.
[14] S. Okahisa, K. Nakayama, Y. Nakayama, Y. Ishii, and M. Fukuda, "Guiding Properties of 1.31- and 1.55-μm-Wavelength Surface Plasmon Polaritons on Striped Waveguides on Silicon and their Wavelength-Selective Detection," J. Lightwave Technol., vol. 35, pp. 2702-2711, 2017.
[15] T. Aihara, M. Fukuda, "Transmission properties of surface- plasmon-polariton coherence," Appl. Phys. Lett., vol. 100, Art No. 213115, 2012.
[16] T. Aihara, H. Sakai, A. Takeda, S. Okahisa, M. Fukuhara, M. Ota, Y. Ishii, and M. Fukuda, "Coherent Plasmonic Interconnection in Silicon-Based Electrical Circuit," J. Lightwave Tech., vol. 33, pp. 2139-2145, 2015.
[17] T. Aihara, K. Nakagawa, M. Fukuhara, Y. L. Yu, K. Yamaguchi, and M. Fukuda, "Optical frequency signal detection through surface plasmon polariton," Appl. Phys. Lett., vol. 99, Art. No. 043111, 2011.
[18] A. Takeda, T. Aihara, M. Fukuhara, Y. Ishii, and M. Fukuda, "Schottky-type surface plasmon detector with nano-slit grating using enhanced resonant optical transmission," J. Appl. Phys., vol. 116, Art. No. 084313, 2014.
[19] J. S. Helman and F. Sa`nchez-Sinencio, "Theory of internal photoemission," Phys. Rev. B, vol. 7, pp. 3702–3706, 1973.
[20] M. Casalino, L. Sirleto, M. Iodice, N. Saffioti, M. Gioffre`, I. Rendina, and G. Coppola, "Cu/p-Si Schottky barrier-based near infrared photodetector integrated with a silicon-on-insulator waveguide," Appl. Phys. Lett., vol. 96, Art. No. 241112, 2010.
[21] S. Zhu, G. Q. Lo, and D. L. Kwong, "Theoretical investigation of silicide Schottky barrier detector integrated in horizontal metal-insulator-silicon-insulator-metal nanoplasmonic slot waveguide," Opt. Exp., vol. 19, pp. 15843–15854, 2011.
[22] I. Goykhman, B. Desiatov, J. Khurgin, J. Shappir, and U. Levy, "Waveguide based compact silicon Schottky photodetector with enhances responsivity in the telecom spectral band," Opt. Exp., vol. 20, pp. 28594–28602, 2012.
[23] B. Steinberger, A. Hohenau, H. Ditlbacher, A. L. Stepanov, A. Drezet, F. R. Aussenegg, A. Leitner, and J. R. Krenn, "Dielectric stripes on gold as surface plasmon waveguides," Appl. Phys. Lett. vol. 88, Art. No. 094104, 2006.
[24] X. Shi, X. Zhang, Z. Han, U. Levy, and S. I. Bozhevolnyi, "CMOS-Compatible Long-Range Dielectric -Loaded Plasmonic Waveguides," J. Lightwave Tech., vol. 31, 3361-3367, 2013.
[25] M. Stockman, "Nanofocusing of Optical Energy in Tapered Plasmonic Waveguides," Phys. Rev, Lett., vol. 93, Art. No. 137404, 2004.
[26] J. Takahara, and F. Kusunoki, "Guiding and nanofocusing of two-dimensional optical beam for nanooptical integrated circuits," IEICE Trans. Electron., vol. E90-C, pp. 87-94, 2007.
[27] M. Fukuhara, M. Ota, A. Takeda, T. Aihara, H. Sakai, Y. Ishii, and M. Fukuda, "Surface-Plasmon Waveguides as Transmission Lines for Optical Signal and Electrical Bias," J. Lightwave Tech., vol. 32, pp. 4490-4495, 2014.